A new Path Planner based on Flatness Approach Application to an Atmospheric Reentry Mission

Vincent Morio, Franck Cazaurang, Ali Zolghadri, and Philippe Vernis

Abstract— **This communication proposes a method for designing a model-based onboard path planner for next generation reusable launch vehicles. Flatness approach is used to map the system dynamics into a lower dimension space. As a consequence, the number of optimization variables associated to the optimal control problem is reduced. In addition, nonconvex nonlinear trajectory constraints in the flat output space are inner approximated by means of deformable geometric shapes. A genetic algorithm is used to find a global solution both for the geometric shapes and the associated geometric transformations tuning parameters. Finally, simulations results, based on the terminal area energy management phase of the Shuttle orbiter STS-1 reentry mission, are presented to illustrate the proposed approach.**

Index Terms— **trajectory planning, differential flatness, convexification, genetic algorithm, superquadrics.**

I. Introduction

Today, trajectory generation for reusable launch vehicles (RLV) requires a significant amount of pre-flight analysis. Depending on the type of mission, ground intervention could be too complex, too long or temporarily impossible (i.e., in case of automated operation during a critical phase), and/or too costly. Reliable onboard path planning appears to be a promising alternative, as it could provide a greater flexibility to account for off-nominal conditions or even to recover timely the vehicle from faulty situations.

The motivation behind this work is to provide a general and efficient method for onboard path planning of RLV. The main advantage over the existing strategies is that the initial optimal control problem, formulated in the state space, is transformed into a convex geometric setup by using flatness approach and annexation techniques, leading to an integration-free programming problem, computationally tractable and that can be solved quickly. The concept of differential flatness has been widely used in the framework of trajectory generation [1]. The main objective is to minimize the number of decision variables involved in the optimal control problem (OCP) by mapping the nonlinear system dynamics to a lower dimensional space. However, flatness parametrization does not preserve the convexity of the initial optimal control problem. In [2], the authors conclude that if the number of optimization variables is decreased while maintaining convexity, computational burden could be significantly reduced. It would be of great interest to keep the flat formulation to provide a minimum number of optimization variables, while at the same time ensuring the convexity of the OPC in the flat output space. In [3], a technique called polyhedral annexation has been introduced, which consists in enlarging a polytope by annexing more and more portions of the nonconvex feasible set associated to some nonlinear trajectory constraints. However, although polytopes provide exibility by a large variety of reachable shapes, they become very difficult to handle in high order spaces, the computation of their volumes being a NP-hard problem. Recently, some results about convexification by n-D superquadric shapes have been obtained in [4], which constitute the starting point of this work.

The contribution of this paper can be summarized as follows. First, flatness property of the guidance model is proved, and the original optimal control problem is transformed into a geometric and integration-free framework. Next, a general and efficient methodology is proposed to inner approximate a set of nonconvex nonlinear constraints, by a smooth convex one. Finally, a genetic algorithm (GA) is used to find a global solution both for the superquadric shapes and the associated geometric transformations tuning parameters. The overall method is then applied to the terminal area energy management phase of the Shuttle orbiter atmospheric reentry mission.

The remainder of the paper is organized as follows. Section 2 briefly presents the interest of differential flatness for trajectory generation. Then, the proposed superellipsoidal convexification method is described in section 3. In section 4, the proposed path planning method is applied, step by step, to the terminal area energy management (TAEM) phase of an atmospheric reentry mission. Some concluding remarks are given in a final section.

II. Differential flatness and trajectory generation

A. Brief review of differential flatness

Differential flatness has been introduced in early 90's [5] and has been applied to a wide number of problems since then. The main interest behind this concept lies in the ability to transform the nonlinear model of a process into a trivial one, i.e., a chain of pure integrators. More precisely, we

V. Morio, F. Cazaurang and A. Zolghadri are with Automatic Control Department, Bordeaux University, IMS Lab, 351 cours de la Libération, 33405 Bordeaux, France, e-mails: vincent.morio@ims-bordeaux.fr, franck.cazaurang@ims-bordeaux.fr, ali.zolghadri@ims-bordeaux.fr

P. Vernis is with Guidance and Control Systems Department, Astrium Space Transportation, 66 route de Verneuil, 78133 Les Mureaux, France. e-mail: philippe.vernis@astrium.eads.net

ISBN 978-963-311-369-1

consider a general dynamic system given by

$$\dot{x} = f(x, u), \tag{1}$$

where x is the n-dimensional state vector, u the m-dimensional input vector, and $f(.)$ is a smooth nonlinear function. We assume that$m \leq n$, which means that the set of equations is underdetermined[1].

Definition 1 (Differential flatness [5]): The nonlinear system (1) is (differentially) *flat* if and only if there exists a collection of smooth nonlinear functions $z = (z_1, \ldots, z_m)$ such that:

- z and its successive derivatives $\dot{z}, \ddot{z}, \ldots$, are differentially independent,
- $z = \Phi\left(x, u, \dot{u}, \ldots, u^{(\alpha)}\right)$ is called a *flat output*,
- Conversely, x and u can be expressed as

$$\begin{cases} x = \Psi_x\left(z, \dot{z}, \ldots, z^{(\beta-1)}\right), \\ u = \Psi_u\left(z, \dot{z}, \ldots, z^{(\beta)}\right), \end{cases} \tag{2}$$

where $\beta = (\beta_1, \ldots, \beta_m)$ is a finite m-tuple of integers. Thus, trajectories of the nonlinear flat system (1) are equivalent to those of the trivial system $z^{(\beta)} = v$.

B. Optimal control problem in the flat output space

It is assumed that all the path planning requirements, defined either at mission or vehicle levels, may be integrated into a general optimal control problem (OCP) defined by:

$$\begin{aligned} \min_{x(t),u(t)} \quad & \mathcal{C}_0\left(x(t_0), u(t_0)\right) + \int_{t_0}^{t_f} \mathcal{C}_t\left(x(t), u(t)\right) dt \\ & + \mathcal{C}_f\left(x(t_f), u(t_f)\right) \end{aligned} \tag{3}$$

s.t.

$$\begin{array}{rcccl} & & \dot{x}(t) = f\left(x(t), u(t)\right), & & t \in [t_0, t_f], \\ l_0 & \leq & A_0 x(t_0) + B_0 u(t_0) & \leq & u_0, \\ l_t & \leq & A_t x(t) + B_t u(t) & \leq & u_t, \quad t \in [t_0, t_f], \\ l_f & \leq & A_f x(t_f) + B_f u(t_f) & \leq & u_f, \\ L_0 & \leq & c_0\left(x(t_0), u(t_0)\right) & \leq & U_0, \\ L_t & \leq & c_t\left(x(t), u(t)\right) & \leq & U_t, \quad t \in [t_0, t_f], \\ L_f & \leq & c_f\left(x(t_f), u(t_f)\right) & \leq & U_f, \end{array}$$

where $\mathcal{C}_0$, $\mathcal{C}_t$ and $\mathcal{C}_f$ are appropriate cost functions, (l_0, u_0), (l_t, u_t) and (l_f, u_f) represent respectively lower and upper bounds on *linear* initial, trajectory and final constraints, and (L_0, U_0), (L_t, U_t) and (L_f, U_f) are lower and upper bounds on *nonlinear* initial, trajectory and final constraints. The transcription of the optimal control problem (3) into an nonlinear programming problem (NLP) in the flat output space is carried out in two stages: 1) parametrization of the flat output components $\{z_i\}_{i=1}^m$ by piecewise polynomial functions (B-splines) such that

$$z_i^{(r)}(t, p_0, \ldots, p_{N_c-1}) = \sum_{j=0}^{N_c-1} \mathcal{B}_{j,d}(t) p_j, t \in [t_0, t_f], \tag{4}$$

where $\mathcal{B}_{j,d}^{(0)}(t)$ is the jth B-spline basis function of degree d, built on a given knot sequence, and p_j is the corresponding jth control point [6], 2) balanced discretization in the time parameter.

[1]note that, by definition, the number of flat output components is equal to the number of system inputs [5].

This formulation is obtained by using flatness property which make it possible to get an integration-free formulation by removing the dynamic constraints. The equivalent optimal control problem can be rewritten in the flat output space as

$$\min_{\overline{z}(t)} \quad \mathcal{G}_0\left(\overline{z}(t_0)\right) + \int_{t_0}^{t_f} \mathcal{G}_t\left(\overline{z}(t)\right) dt + \mathcal{G}_f\left(\overline{z}(t_f)\right) \tag{5}$$

s.t.

$$\begin{array}{rcccl} l_0 & \leq & A_0 \overline{z}(t_0) & \leq & u_0, \\ l_t & \leq & A_t \overline{z}(t) & \leq & u_t, \quad t \in [t_0, t_f], \\ l_f & \leq & A_f \overline{z}(t_f) & \leq & u_f, \\ L_0 & \leq & \widetilde{c}_0\left(\overline{z}(t_0)\right) & \leq & U_0, \\ L_t & \leq & \widetilde{c}_t\left(\overline{z}(t)\right) & \leq & U_t, \quad t \in [t_0, t_f], \\ L_f & \leq & \widetilde{c}_f\left(\overline{z}(t_f)\right) & \leq & U_f, \end{array}$$

where $\overline{z} = (z_1, \ldots, z_m, \dot{z}_1, \ldots, \dot{z}_m, \ldots)$ in the infinite order jets space [7]. In next section, a methodology is proposed to get a convex optimal control problem. The technique is based on the inner approximation, by superquadric shapes, of the trajectory constraints and the cost functional included in the OCP (5).

III. Convexification by superquadric shapes

The optimal control problem (5) obtained in the previous section may be directly used to compute an optimal trajectory. However, most of trajectory constraints, once transformed in the flat output space, become highly nonlinear and nonconvex [2]. In this section, a convexification method, based on deformable superquadric shapes and genetic algorithms, is proposed. This process results in a convex OCP, with guaranteed convergence, which can be solved efficiently with improved computational performances.

A. Generalized superquadric shapes

In order to perform a trade-off between complexity (i.e., number of attainable shapes), and numerical tractability in high order flat output spaces, superquadric primitives have been retained to inner-approximate the feasible set associated to nonlinear trajectory constraints. Superquadrics have been introduced in [8] as a generalization in n dimensions of superellipses, and have been applied to a number of problems. The main advantage is that few parameters are needed to describe the overall shape, and also that an explicit representation exists. Thus, this section will focus on the extension in n dimensions of formulas existing only for three-dimensional applications.

Basically, a n-dimensional superquadric shape may be described by the implicit analytical function $\mathcal{F}_n(x) = \Lambda_{n,n}(x)$ given by the following recursive expression:

$$\begin{cases} \Lambda_{n,2}(x) = \left(\frac{x_1}{a_1}\right)^{\frac{2}{\varepsilon_1}} + \left(\frac{x_2}{a_2}\right)^{\frac{2}{\varepsilon_1}}, \\ \Lambda_{n,k}(x) = \left(\Lambda_{n,k-1}(x)\right)^{\frac{\varepsilon_{k-2}}{\varepsilon_{k-1}}} + \left(\frac{x_k}{a_k}\right)^{\frac{2}{\varepsilon_{k-1}}}, \end{cases} \tag{6}$$

where x is the vector of n-dimensional Cartesian coordinates, $a \in \mathbb{R}^n$ the semi-major axes, and $\varepsilon \in \mathbb{R}^{n-1}$ the roundness parameters. The expression $\mathcal{F}_n$, so-called inside-outside function, enjoys the following properties:

- $\mathcal{F}_n(x) < 1$: the point x lies inside the superquadric,
- $\mathcal{F}_n(x) = 1$: the point x lies on the surface of the shape,
- $\mathcal{F}_n(x) > 1$: the point x lies outside the superquadric.

The values of the roundness parameters are used to adjust the convexity of the superquadric shape. It has been proved in [8] that the superquadrics are convex if, $\forall i$, $\varepsilon_i \in]0, 2]$. In order to fully characterize the shapes in n dimensions, some definitions and notations must be introduced first. The n-D extension of the so-called "angle-center" representation [9] provides a near-optimal sampling of the superquadric surface.

Proposition 1 (n-D angle-centre parametrization): Let $\mathcal{S}$ be a n-dimensional superellipsoid, defined by semi-major axes $a \in \mathbb{R}^n$, roundness parameters $\varepsilon \in \mathbb{R}^{n-1}$, and parameterized by anomalies $\theta \in \mathbb{R}^{n-1}$. Then, the corresponding *angle-center parametrization*, with Cartesian coordinates x_i, $i = 1, \ldots, n$, is given by

$$x_i = \begin{cases} r(\theta) \prod_{k=1}^{n-1} \cos\theta_k, & i = 1, \\ r(\theta) \sin\theta_{i-1} \prod_{k=i}^{n-1} \cos\theta_k, & i = 2, \ldots, n-1, \\ r(\theta) \sin\theta_{n-1}, & i = n, \end{cases} \tag{7}$$

where the radius $r(\theta) = \dfrac{1}{\chi_{n,n}}$ is defined by the recursive expression

$$\chi_{n,2} = \left[\left(\frac{\prod_{k=1}^{n-1} \cos\theta_k}{a_1} \right)^{\frac{2}{\varepsilon_1}} + \left(\frac{\sin\theta_1 \prod_{k=2}^{n-1} \cos\theta_k}{a_2} \right)^{\frac{2}{\varepsilon_1}} \right]^{\frac{\varepsilon_1}{2}},$$

$$\chi_{n,j} = \left[(\chi_{n,j-1})^{\frac{2}{\varepsilon_{j-1}}} + \left(\frac{\sin\theta_{j-1} \prod_{k=j}^{n-1} \cos\theta_k}{a_j} \right)^{\frac{2}{\varepsilon_{j-1}}} \right]^{\frac{\varepsilon_{j-1}}{2}},$$

with $\theta_i \in [-\pi, \pi[$ if $i = 1$ and $\theta_i \in [-\frac{\pi}{2}, \frac{\pi}{2}]$ otherwise.

Another important aspect linked to the use of superquadrics concerns the number of attainable shapes, which is limited due to the intrinsically weak number of available degrees of freedom. Therefore, some geometric transformations have been introduced to encompass a wide number of nonconvex nonlinear constraints, namely n-D rotation, translation, and linear pinching along a single axis (not detailed here). Hence, the set Ψ, containing all the sizing parameters needed to obtain a positioned, oriented and bended superquadric shape, is defined by

$$\Psi = \{\underbrace{a_1, \ldots, a_n}_{\text{semi-axes}}, \underbrace{\varepsilon_1, \ldots, \varepsilon_{n-1}}_{\text{roundness}}, \underbrace{\Phi_1, \ldots, \Phi_{n(n+1)/2}}_{\text{rotation}}, \underbrace{d_1, \ldots, d_n}_{\text{translation}}, \underbrace{v_1, \ldots, v_{n-1}}_{\text{pinching}}\}. \tag{8}$$

The inside-outside function (6) has been modified in order to account for the previous n-D transformations.

Proposition 2 (n-D inside-outside function): let $\mathcal{S}$ be a superellipsoid of size n, described by the vector Ψ defined by (8). Then, the (implicit) n-D *inside-outside function* $\mathcal{F}_n(\Psi, x) = \Lambda_{n,n}(\Psi, x)$ is defined by the following recursive expression:

$$\begin{cases} \Lambda_{n,2}(\Psi, x) = \left(\dfrac{x_1}{a_1 \left(\frac{v_1}{a_p} x_p + 1 \right)} \right)^{\frac{2}{\varepsilon_1}} + \left(\dfrac{x_2}{a_2 \left(\frac{v_2}{a_p} x_p + 1 \right)} \right)^{\frac{2}{\varepsilon_1}}, \\ \Lambda_{n,k}(\Psi, x) = \left(\Lambda_{n,k-1}(\Psi, x) \right)^{\frac{\varepsilon_{k-2}}{\varepsilon_{k-1}}} + \left(\dfrac{x_k}{a_k \left(\frac{v_k}{a_p} x_p + 1 \right)} \right)^{\frac{2}{\varepsilon_{k-1}}}, \end{cases} \tag{9}$$

where $v_p = 0$ in the pinching direction p.

Moreover, the volume of a superquadric shape $\mathcal{S}$ of order n can be obtained from the explicit parametrization (1). The superquadric volume will be used in the objective function of the convexification process.

Proposition 3 (n-D superellipsoid volume): Let $\mathcal{S}$ be a bended superellipsoid of size n, described by the vector Ψ defined by (8). The volume $V_n(\Psi)$ of $\mathcal{S}$ is given by (10), where the multi-index $\alpha = (\alpha_1, \ldots, \alpha_{p-1}, 0, \alpha_{p+1}, \ldots, \alpha_n)$ satisfies

$$v^\alpha = \prod_{k=1}^{n} v_k^{\alpha_k}, \quad |\alpha| = \sum_{j=1}^{n} \alpha_j, \quad \alpha_i \in \{0, 1\}, i = 1, \ldots, n.$$

In addition, the Beta function $B(x, y)$ is linked to the Gamma function by

$$B(x, y) = 2 \int_0^{\pi/2} \sin^{2x-1}\phi \cos^{2y-1}\phi d\phi = \frac{\Gamma(x)\Gamma(y)}{\Gamma(x+y)},$$

the Gamma function being typically defined by

$$\Gamma(x) = \int_0^\infty \exp^{-t} t^{x-1} dt.$$

In addition, to avoid numerical issues during the convexification process, a normalized volume $\widetilde{V}_n$ is computed such that

$$\widetilde{V}_n(\Psi) = V_n(\Psi)^{\frac{1}{n}}, \tag{11}$$

where n is the order of the superquadric shape. Assume that the initial nonconvex domain may be described by means of one or more implicit analytical expressions given by

$$f_{min} \leq f_{nc}(x) \leq f_{max},$$

where x is a n-dimensional set of variables. The convexification problem can then be stated as follows.

Problem 1 (superellipsoidal annexion problem): Let $\mathcal{S}$ be a superellipsoid of size n, described by the vector Ψ defined by (8). The *superellipsoidal annexion problem* consists in finding the optimal parameters Ψ^* associated to the largest

$$V_n(\Psi) = 2a_n \left[\prod_{\substack{i=1 \\ i \neq p-1}}^{n-1} a_i \varepsilon_i B\left(\frac{\varepsilon_i}{2}, i\frac{\varepsilon_i}{2} + 1 \right) \right] \cdot \left[a_{p-1}\varepsilon_{p-1} \sum_{|\alpha|=0}^{n-1} v^\alpha B\left(\frac{|\alpha|+1}{2}\varepsilon_{p-1}, \frac{p-1}{2}\varepsilon_{p-1} + 1 \right) \right], \tag{10}$$

ellipsoid $\mathcal{S}_{opt}$ contained inside the nonconvex domain described by f_{nc}, such that

$$\max_{\Psi} \quad \widetilde{V}_n(\Psi) \qquad (12)$$
$$\text{s.t.} \quad \begin{cases} \mathcal{F}_n(\Psi, x) \leq 1, \\ f_{min} \leq f_{nc}(x) \leq f_{max}, \\ x_i^l \leq x_i \leq x_i^u, \quad i = 1, \ldots, n, \end{cases}$$

where the superellipsoid volume $\widetilde{V}_n(\Psi)$ is defined by (11), and the i/o function $\mathcal{F}_n(\Psi, x)$ by (9).
The optimal set of tuning parameters Ψ^* is then found by using a genetic algorithm, which is a robust and global optimization method (see [10] for a survey). As regards Problem 1, the initial population of the GA is generated such that some elementary convex volumes matching the constraints (12) are randomly drawn over the whole search space. Then, near-uniform samplings of the superquadrics surfaces are performed by using the angle-center parametrization given in proposition 1. Each individual fitness consists of two parts: a normalized volume term, which is computed by means of eq. (11), and an inside-outside function constraint violation term, computed by a modified tournament selection operator.

B. Convex optimal control problem

Let us assume that one or several superquadric shapes have been found to be solutions of Problem 1 and let us consider again the OCP (5), described in the flat output space. By using the inside-outside function (2), the nonlinear trajectory constraints and cost functional are replaced by their approximating convex shapes. The goal is then to compute optimal trajectories lying inside the deformable shapes. The optimal control problem becomes:

$$\min_{\overline{z}(t)} \quad \mathcal{G}_0(\overline{z}(t_0)) + \int_{t_0}^{t_f} \mathcal{G}_t(\overline{z}(t))\, dt + \mathcal{G}_f(\overline{z}(t_f)) \qquad (13)$$
s.t.
$$\begin{array}{rcccl} l_0 & \leq & A_0\overline{z}(t_0) & \leq & u_0, \\ l_t & \leq & A_t\overline{z}(t) & \leq & u_t, \quad t \in [t_0, t_f], \\ l_f & \leq & A_f\overline{z}(t_f) & \leq & u_f, \\ L_0 & \leq & \widetilde{c}_0(\overline{z}(t_0)) & \leq & U_0, \\ 0 & \leq & \mathcal{F}_n(\Psi^*, z(t)) & \leq & 1, \quad t \in [t_0, t_f], \\ L_f & \leq & \widetilde{c}_f(\overline{z}(t_f)) & \leq & U_f. \end{array}$$

Remark 1: It should be noted that the trajectory endpoints constraints $\mathcal{F}_n(\Psi^*, z(t_0)) \leq 1$ and $\mathcal{F}_n(\Psi^*, z(t_f)) \leq 1$ must also be met.
The last step consists in discretizing the convex optimal control problem (13) in order to make it finite-dimensional. For this purpose, consider the uniform time partition

$$t_0 = \Delta_0 < \Delta_1 < \Delta_{N_\Delta - 1} = t_f,$$

where N_Δ is a predefined number of collocation points. The result of the previous discretization is a nonlinear programming problem (NLP) where the unknowns are the active control points of all B-spline curves. The corresponding nonlinear programming problem can then be solved by using a dedicated solver.

IV. Application to Terminal Area Energy Management Path Planning

A. Description of the TAEM reentry phase

The terminal area management phase is principally aimed at dissipating the total energy of the vehicle. The flight segment begins at the TAEM entry point (TEP), at the end of the hypersonic phase, and extends to the approach/landing capture zone, at the nominal energy point (NEP), defined when the vehicle is on glideslope, on airspeed, and on extended runway centerline (see Fig. 1). The path planning requirements during the TAEM flight segment are threefold. First, protection against excessive mechanical constraints (essentially the load factor and dynamic pressure) must be ensured. Second, final path constraints dictated by kinematic conditions at NEP must be met in order to ensure a safe autolanding. Third, to avoid possible actuator saturations in the flight control loop, guidance commands must remain within prescribed ranges. The main objective of the guidance software is then to generate the necessary commands to enable the vehicle to achieve the proper A&L conditions, while taking into account various energy conditions due to dispersions at TEP. The reader can found more details about TAEM guidance in [11], [12].

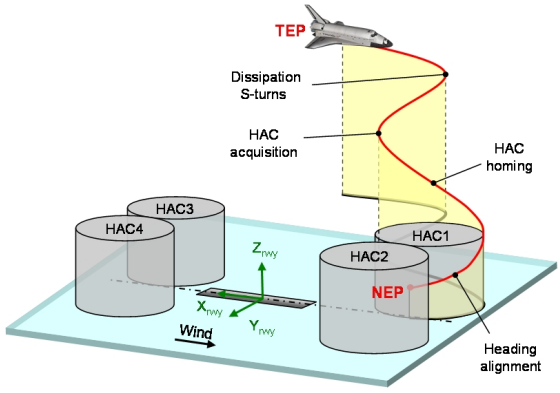

Fig. 1. Typical TAEM path

B. Flatness property of the guidance model

Under the assumption of a non-rotating Earth, which is licit with respect to the trajectory sizing, the vehicle can be located in a Lambert conformal conic projection frame (flat Earth coordinates) linked to the runway center $(X_{rwy}, Y_{rwy}, Z_{rwy})$ [13]. Moreover, it is assumed that symmetric flight condition exists in the baseline guidance scheme, i.e., $\beta = 0$. Such a requirement is compliant with the path planning objectives. Moreover, as time is not a relevant parameter during atmospheric entry, a free trajectory duration parameter λ is considered, the latter being strictly monotonic along the TAEM trajectory. Introducing the normalized time $\tau = \frac{t}{\lambda}$ with $0 \leq \tau \leq 1$, then $d(.)/d\tau = \lambda \frac{d(.)}{dt} = (.)'$, and the

point-mass equations become:

$$x' = \lambda V \cos\chi \cos\gamma, \quad (14)$$
$$y' = \lambda V \sin\chi \cos\gamma, \quad (15)$$
$$h' = \lambda V \sin\gamma, \quad (16)$$
$$V' = \lambda\left(-\frac{D}{m} - g\sin\gamma\right), \quad (17)$$
$$\gamma' = \lambda\left(\frac{L\cos\mu}{mV} - \frac{g}{V}\cos\gamma\right), \quad (18)$$
$$\chi' = \lambda\frac{L\sin\mu}{mV\cos\gamma}, \quad (19)$$

where $(x, y, h, V, \gamma, \chi)$ is the state (x is the downrange, y the crossrange, h the altitude, V the relative velocity, γ the flight path angle and χ the heading) and (α, μ) the guidance commands (α is the angle-of-attack and μ the aerodynamic bank angle). The terms L and D denote respectively the lift and drag forces, depending on the aerodynamic coefficients in clean configuration such as

$$L(\alpha, M) = \frac{1}{2}\rho S V^2 C_L(\alpha, M), \quad (20)$$
$$D(\alpha, M) = \frac{1}{2}\rho S V^2 C_D(\alpha, M). \quad (21)$$

The aerodynamic coefficients must be approximated by smooth continuous analytic functions so as to invert the nonlinear guidance equations properly. In clean configuration, the coefficients are provided by 2-dimensional look-up tables extracted from the open-source Shuttle Orbiter STS-1 aerodynamic design data book[2] A fitting technique is then used, based on principal component analysis and neural networks (not detailed here). Finally, a simple atmospheric model is considered, with a constant gravitational acceleration and an exponential atmospheric density model given by

$$\rho = \rho_0 exp\left(-h/H_{ref}\right), \quad (22)$$

where ρ_0 is the atmospheric density at sea level and H_{ref} is a Earth-relative constant atmospheric scale height tuned for low atmosphere layers.

By choosing $z_1 = x$, $z_2 = y$ and $z_3 = h$ as candidate flat outputs, it can be easily proved that the nonlinear guidance model is not flat, since it is not fully actuated [14]. However, the state and the inputs of the nonlinear point-mass model can be rewritten exclusively as functions of the independent variable λ, the flat outputs and a finite number of their time derivatives. Namely, the states are given by:

$$V = \frac{\sqrt{z_1'^2 + z_2'^2 + z_3'^2}}{\lambda}, \quad (23)$$
$$\gamma = \arctan\left(\frac{z_3'}{\sqrt{z_1'^2 + z_2'^2}}\right), \quad (24)$$
$$\chi = \arctan\left(\frac{z_2'}{z_1'}\right), \quad (25)$$
$$(26)$$

[2]freely available on NASA website at http://ntrs.nasa.gov.

and the control inputs are obtained from (18)-(19) as

$$\mu = \arctan\left(\frac{\chi'\cos\gamma}{\gamma' + \frac{g\cos\gamma}{V}\lambda}\right), \quad (27)$$
$$\alpha = \frac{2m\cos\gamma\chi'}{a_1 f_{CL}(M)\rho S V \lambda \sin\mu} - \frac{a_0}{a_1}. \quad (28)$$

However, since the model (14)-(19) is not flat with $\beta = 0$, the following equality constraint must also be satisfied along the TAEM path:

$$\frac{V'}{\lambda} + g\sin\gamma + \frac{1}{2}\frac{\rho S V^2 C_D(\alpha, M)}{m} = 0. \quad (29)$$

C. Convexification of nonlinear trajectory constraints

We consider the dynamic pressure constraint Q, expressed as a function of the flat outputs, which must be lower than $Q_{max} = 16$ kPa along the reference TAEM trajectory, i.e.,

$$0 \leq \frac{1}{2}\rho_0 \exp -\frac{z_3}{H_{ref}} S \frac{\sqrt{z_1'^2 + z_2'^2 + z_3'^2}}{\lambda} \leq Q_{max}. \quad (30)$$

From a geometrical point of view, this constraint can be viewed as an exponentially contracting spherical shape, the free trajectory duration parameter λ acting as a homothety factor. In order to inner-approximate the dynamic pressure constraint by a convex shape, we consider a 5th order superquadric and the associated 5-D geometric transformations introduced in section III. The superellipsoidal annexion problem 1 has been solved by a genetic algorithm with simple tuning parameters. A projection of the resulting superquadric shape in the $(z_1'\lambda, z_3, z_2'\lambda)$ frame is depicted in Fig. 2 as well as the corresponding angle-center parametrization. The same

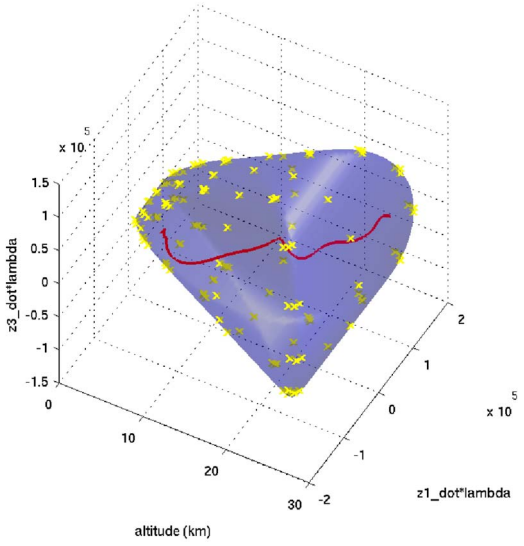

Fig. 2. Inner approximation of the dynamic pressure constraint.

convexification process has also been applied to other nonlinear trajectory constraints such as bank angle, angle-of-attack and load factor.

In order to solve the convex OCP (13), the flat outputs have been parameterized by 7th order B-splines with 5 intervals, and multiplicities of 3 to obtain continuous 1st and 2nd order time derivatives. Then, the OCP (13) has been transformed into a nonlinear programming problem by means of the Nonlinear Trajectory Generation (NTG) software [15]. Finally, the resulting NLP problem has been solved with NPSOL in about 200 ms on a 2Go Intel Core 2 Duo processor. The optimal TAEM trajectory is depicted in Fig. 3, where the load factor constraint, which must not exceed $\Gamma_{max} = 2$ g, is displayed in color. The same trajectory has been projected inside the superquadric shape associated to the dynamic pressure constraint (see Fig. 2). The bank angle and angle-of-attack profiles are

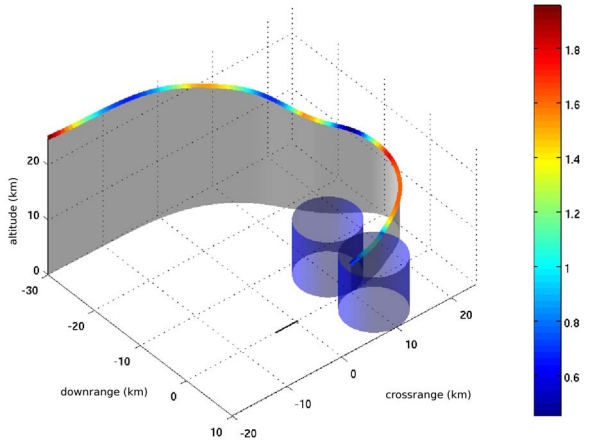

Fig. 3. Reference TAEM trajectory.

depicted in Fig. 4. The guidance commands remain within the prescribed ranges defined by the superquadric shapes. Finally, the mechanical constraints undergone by the vehicle

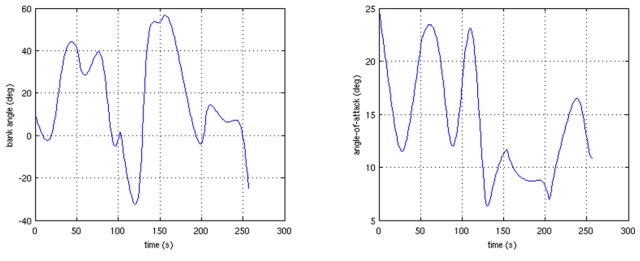

(a) (b)

Fig. 4. (a) Bank angle profile (b) Angle-of-attack profile.

during the TAEM phase are depicted in Fig. 5.

V. Conclusion

The problem studied by this paper is that of designing an efficient model-based onboard path planner for atmospheric reentry vehicles. A convex optimal control problem is formulated by using flatness approach and annexion techniques.

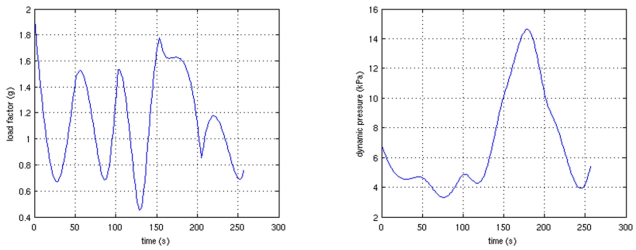

(a) (b)

Fig. 5. (a) Load factor constraint ($\Gamma_{max} = 2$ g) (b) Dynamic pressure constraint ($Q_{max} = 16$ kPa).

The resulting nonlinear programming problem can be solved quickly, with low computational burden. Simulation results have shown the potential of the proposed approach for the terminal area energy management phase of the Shuttle orbiter STS-1 reentry mission. An appealing direction for further work is to make the path planner tolerant to potential single/multiple actuator faults occurring during the reentry mission. This is a topic of our current research.

References

[1] N. Petit, M. Milam, and R. Murray, "Inversion based trajectory optimization," in *Proc. 5th IFAC Symposium on Nonlinear Control Systems Design (NOLCOS)*. St. Petersburg, Russia: IFAC, jul 2001.

[2] I. Ross and F. Fahroo, "Issues in the real-time computation of optimal control," *Mathematical and computer modelling*, vol. 43, no. 9-10, pp. 1172–1188, 2006.

[3] N. Faiz, S. Agrawal, and R. Murray, "Trajectory planning of differentially flat systems with dynamics and inequalities," *Journal of Guidance, Control and Dynamics*, vol. 24, no. 2, pp. 219–227, 2001.

[4] C. Louembet, F. Cazaurang, A. Zolghadri, C. Pittet, and C. Charbonnel, "Design of algorithms for satellite slew maneuvers by flatness and collocation," in *American Control Conference*, 2007.

[5] M. Fliess, J. Lévine, P. Martin, and P. Rouchon, "Flatness and defect of non-linear systems: introduction theory and examples," *Int. Journal of Control*, vol. 61, pp. 1327–1361, 1995.

[6] C. de Boor, *A pratical guide to spline*, ser. Applied Mathematical Sciences. New York: Springer, 2001.

[7] J. Lvine, "On necessary and sufficient conditions for differential flatness," *arXiv*, no. 0605405, 2006.

[8] A. Barr, "Superquadrics and angle-preserving transformations," *IEEE Computer Graphics and Applications*, vol. 1, no. 1, pp. 11–23, jan 1981.

[9] H. Löffelmann and E. Gröller, "Parameterizing superquadrics," in *Third International Conference in Central Europe in Computer Graphics and Visualisation*, Plzen, Czech Republic, 1995, pp. 162–172.

[10] D. Goldberg, *Genetic Algorithms in Search, Optimization, and Machine Learning*. Addison-Wesley Professional, January 1989.

[11] T. Moore, "Space shuttle entry terminal area energy management," no. NASA TM 104744, 1991.

[12] J. Harpold and C. Graves, "Shuttle entry guidance," in *25th Anniversary Conference,American Astronautical Society*, R. A. Metzler and W. F. Powers, Eds., oct 1978.

[13] N. X. Vinh, A. Busemann, and R. D. Culp, *Hypersonic and Planetary Entry Flight Mechanics*. The university of Michigan Press, 1980.

[14] T. Neckel, C. Talbot, and N. Petit, "Collocation and inversion for a reentry optimal control problem," in *Proceedings of the 5th Intern. Conference on Launcher Technology*, 2003.

[15] M. Milam, K. Mushambi, and R. Murray, "A new computational approach to real-time trajectory generation for constrained mechanical systems," in *Proc. 39th IEEE Conference on Decision and Control*. Sydney, Australia: IEEE, 2000.